

Synthesis, Biological Evaluation and Molecular Modeling Studies of *N*-aryl-2-arylthioacetamides as Non-nucleoside HIV-1 Reverse Transcriptase Inhibitors

Zhu Xiaohe, Qin Yu, Yan Hong*,
Song Xiuqing and Zhong Rugang

College of Life Science and Bio-engineering, Beijing University of Technology, Pingleyuan Street No. 100, Chaoyang District, Beijing 100124, China

*Corresponding author: Yan Hong, hongyan@bjut.edu.cn

A series of *N*-aryl-2-arylthioacetamide derivatives (2–4) designed as non-nucleoside reverse transcriptase inhibitors was synthesized and evaluated for their inhibitory activity against HIV-1 (IIIB) replication in MT-4 cell cultures. The compounds 2–4 were performed by the reaction of thiols and 2-chloro-*N*-substituted-acetamides and active in the lower micromolar concentration (1.25–20.83 μ M). The studies of structure–activity relationship suggested that 1*H*-benzo[*d*]imidazole ring at arylthio moiety strongly improved the anti-HIV activity and consistent with the experimental data. The results of molecular modeling and docking within the RT non-nucleoside binding site using AutoDock confirmed that the 3 series, similar to other non-nucleoside reverse transcriptase inhibitors such as *N*-(5-chloro-2-pyridinyl)-*N'*-[2-(4-ethoxy-3-fluoro-2-pyridinyl)ethyl]-thiourea (PETT), was assumed in a butterfly-like conformation and helped to rationalize some SARs and the biological activity data.

Key words: antiviral agents, molecular docking, *N*-aryl-2-arylthioacetamides, non-nucleoside reverse transcriptase inhibitors, structure–activity relationships

Received 31 January 2010, revised 7 June 2010 and accepted for publication 16 June 2010

HIV-1 reverse transcriptase (RT) is an essential enzyme converting the single-stranded viral RNA genome into linear double-stranded DNA prior to its integration into the host genomic DNA (1). Because of its important role in the HIV-1 life cycle, RT is one of the most attractive targets for the development of new antiretroviral agents (2–4). Two functionally distinct classes of HIV-1 RT inhibitors have been discovered and used in clinically or clinical trials (5,6): nucleoside reverse transcriptase inhibitors (NRTIs) that interact competitively with the catalytic site of the RT, and non-nucleoside reverse

transcriptase inhibitors (NNRTIs) that inhibit the enzyme by an allosteric interaction with a site adjacent to the NRTI binding site (the non-nucleoside inhibitor binding site, namely NNBS). Non-nucleoside reverse transcriptase inhibitors have gained an increasingly important role in the therapy of HIV infection in multidrug regimens and highly active antiretroviral therapy (HAART), such as nevirapine, delavirdine, efavirenz (7–9), 4,5,6,7-tetrahydroimidazo[4,5,1-*j*][1,4]benzodiazepin-2(1*H*)-one and -thione (TIBO) derivatives (10), thiocarboxanilides (11) and pyridinones (12). However, the emergence of drug-resistant viral strains (13–15) has limited the therapeutic efficiency of these inhibitors. Therefore, there is an urgent need to develop novel classes of NNRTIs with activity against the drug-resistant mutants.

Recently, a novel class of HIV-1 NNRTIs, *N*-aryl-2-arylthioacetamides, e.g.: sulfanyltriazoles **A** (16), sulfanyltetrazoles **B** (17), sulfanylthiadiazoles **C** (18) and VRX-480773 (19), has been identified by the submicromolar activity and significant *in vitro* activity, especially the VRX-480773 inhibited viruses from efavirenz-resistant molecular clones (Figure 1). Studies of crystal structures of the RT complex with inhibitors suggested that NNRTIs share a common mode of action and interact with a hydrophobic pocket. Upon binding, *N*-aryl-2-arylthioacetamides assumed a typical butterfly-like conformation, the arylthio moiety and the phenyl ring mimicking the butterfly wings. Structure–activity relationship (SAR) studies showed that the arylthio moiety strongly influenced the antiviral activity, leading to different results depending on steric/electronic properties of atoms/groups. Furthermore, introduction of a set of electron-withdrawing groups at *N*-aryl moiety was highly positive for anti-HIV-1 activity. On the basis of these mode, the lead compounds (Figure 1) had been mainly based on independent variations of the portions and established the potent derivatives **2–4** (Figure 2) featured by the following patterns: (i) the substitution of pyridine, 1*H*-benzo[*d*]imidazole and 1,3,4-thiadiazole rings at arylthio moiety, (ii) the substitution of the phenyl ring or replacement of the phenyl ring with a pyrimidyl ring at *N*-aryl moiety.

In this study, we described a facile synthesis of *N*-aryl-2-arylthioacetamide derivatives **2–4** and an evaluation for their inhibitory activity against HIV-1 (IIIB). With the aim to rationalize the biological results and to predict the activity of novel NNRTIs of **2–4**, we focused on the SAR and the correlation between the inhibitory activities and the binding free energies, obtained by structural and

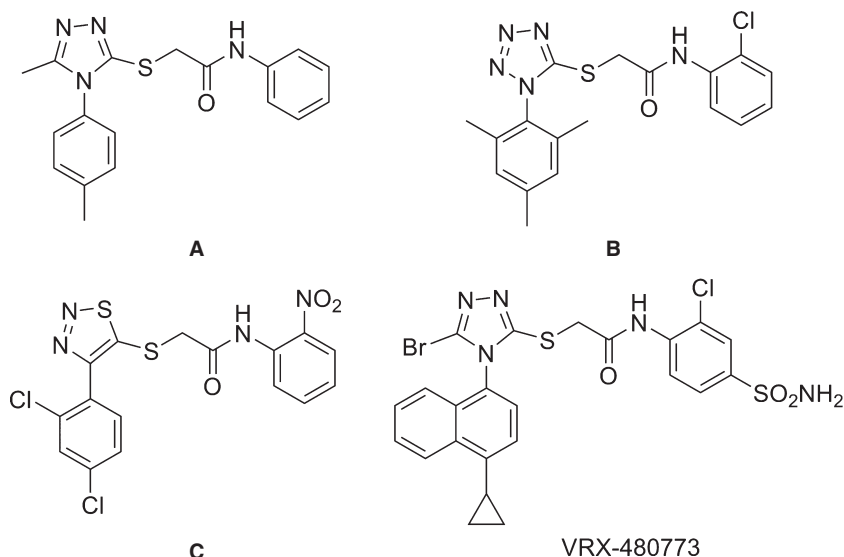


Figure 1: Lead *N*-aryl-2-arylthioacetamide inhibitors of HIV-1 RT.

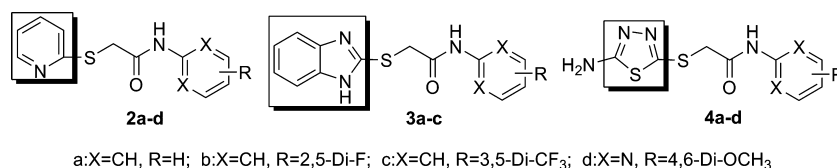


Figure 2: Novel synthesized *N*-aryl-2-arylthioacetamide derivatives.

molecular modeling studies on the HIV-1 RT NNBS using AutoDock 4.0 (Scripps Research Institute, La Jolla, CA, USA).

Methods and Materials

Melting points were determined on a XT-4A melting point apparatus and were uncorrected. Infrared (IR) spectra (KBr) were recorded on a Bruker vertex 70 spectrophotometer. ¹H NMR spectra were obtained using a Bruker ARX-400 MHz spectrophotometer, and chemical shift values are expressed in δ values (ppm) relative to tetramethylsilane (TMS) as internal standard. Coupling constants are given in Hz, and signals are quoted as follows: s (singlet), d (doublet), t (triplet), m (multiplet) and br s (broad singlet). All NH and OH protons were exchangeable with D₂O. Electrospray ionization mass spectra (ESI-MS) were measured on a ZAB-HS & ESQUIRE6000 mass spectrometer. All compounds were routinely checked by TLC and ¹H NMR. TLC was performed by using aluminum-baked silica gel plates (60 HF-254, Combinol Reagent Corp., Yantai, China). The developed chromatograms were visualized under ultraviolet light at 254 nm or by iodine vapor. All solvents were reagent grade and, when necessary, were purified and dried by standard methods.

General procedures for the preparation of 2-chloro-*N*-substituted-acetamides (1)

Chloroacetyl chloride (33.0 mmol) was added dropwise to a mixture of the appropriate amine (28.0 mmol) and acetic acid (25 mL) at

0 °C. The reaction mixture was stirred at room temperature for an additional four hours. Then, it was slowly poured into 100 mL of ice water. The aqueous solution was extracted with CH₂Cl₂ (2 × 100 mL), the organic phase was washed and dried over Na₂SO₄, filtered and the solvent was evaporated to furnish a solid residue which was purified by crystallization from a mixture of ethyl acetate/petroleum ether.

2-Chloro-*N*-phenylacetamide (1a)

Yield 91.3%; m.p. 129.7–130.9 °C; ¹H NMR (400 MHz, CDCl₃): δ (ppm) 4.17 (s, 2H, CH₂), 7.20 (m, 1H, PhCH-*p*, *J* = 7.2 Hz), 7.39 (m, 2H, PhCH-*m*, *J* = 7.8, 1.9 Hz), 7.54 (m, 2H, PhCH-*o*, *J* = 7.5, 1.2 Hz), 8.30 (br s, 1H, NH).

2-Chloro-*N*-(2,5-di-fluoro-phenyl)acetamide (1b)

Yield 87.0%; m.p. 116.5–117.6 °C; ¹H NMR (400 MHz, CDCl₃): δ (ppm) 4.19 (s, 2H, CH₂), 6.80 (m, 1H, PhCH-*p*, *J* = 5.6 Hz), 7.20 (m, 1H, PhCH-*m*, *J* = 6.2 Hz), 7.54 (m, 1H, PhCH-*o*, *J* = 2.1 Hz), 9.35 (br s, 1H, NH).

2-Chloro-*N*-(3,5-di-trifluoromethyl-phenyl)acetamide (1c)

Yield 94.8%; m.p. 85.4–86.5 °C; ¹H NMR (400 MHz, CDCl₃): δ (ppm) 4.14 (s, 2H, CH₂), 7.68 (s, 1H, PhCH-*p*), 8.22 (s, 2H, PhCH-*o*), 9.48 (br s, 1H, NH).

2-Chloro-N-(4,6-dimethoxy-pyrimidin-2-yl)acetamide (1d)

Yield 74.9%; m.p. 158.3–159.8 °C; ¹H NMR (400 MHz, CDCl₃): δ (ppm) 3.91 (s, 6H, 2 × OCH₃), 4.26 (s, 2H, CH₂), 5.76 (s, 1H, Pyrimidine-H₅), 9.62 (br s, 1H, NH).

General procedures for the preparation of N-aryl-2-arylthioacetamide derivatives (2–4)

The corresponding thiol (11.7 mmol) was added to a solution of NaOH (0.56 g, 14.1 mmol) in water (5 mL) while stirring at room temperature. A solution of respective 2-chloro-N-substituted-acetamide **1a–d** (9.8 mmol) in ethanol (20 mL) and KI (0.5 g, 3.0 mmol) was added dropwise. Stirring was continued for 1 h, the solvent was removed under reduced pressure, and the residue was treated with water (50 mL) and CH₂Cl₂ (30 mL). The phases were separated and the aqueous layer was extracted with CH₂Cl₂ (2 × 30 mL). The combined organic phases were dried and concentrated to give a solid, then recrystallized from a mixture of CH₂Cl₂/petroleum ether.

N-phenyl-2-(pyridin-2-ylthio)acetamide (2a)

Yield 87.5%; m.p. 61.3–62.9 °C; IR(KBr, cm⁻¹): 3436 (NH), 1684 (C = O); ¹H NMR (400 MHz, CDCl₃): δ (ppm) 3.90 (s, 2H, -CH₂), 7.05–7.09 (t, 1H, PhCH-*p*, *J* = 7.4 Hz), 7.14–7.17 (q, 1H, Pyridine-H₅, *J* = 5.2 Hz), 7.27–7.33 (m, 3H, PhCH-*m*, Pyridine-H₃), 7.49–7.50 (d, 2H, PhCH-*o*, *J* = 8.0 Hz), 7.58–7.62 (m, 1H, Pyridine-H₄, *J* = 7.6 Hz), 8.55–8.56 (t, 1H, Pyridine-H₆, *J* = 4.0 Hz), 10.13 (s, 1H, NH); MS (ESI) *m/z* (%): 266.9 [M+Na]⁺.

N-(2,5-di-fluoro-phenyl)-2-(pyridin-2-ylthio)acetamide (2b)

Yield 50.6%; m.p. 112.5–113.8 °C; IR(KBr, cm⁻¹): 3435 (NH), 1694 (C = O); ¹H NMR (400 MHz, CDCl₃): δ (ppm) 3.90(s, 2H, -CH₂), 6.65–6.69 (m, 1H, Ph-H₄), 6.93–6.99 (m, 1H, Ph-H₃), 7.13–7.16 (m, 1H, Ph-H₆), 7.29–7.32 (d, 1H, Pyridine-H₅, *J* = 8.4 Hz), 7.57–7.61 (m, 1H, Pyridine-H₃), 8.21–8.26 (m, 1H, Pyridine-H₄), 8.54–8.55 (t, 1H, Pyridine-H₆, *J* = 2.4 Hz), 10.85 (s, 1H, NH); MS (ESI) *m/z* (%): 302.9 [M+Na]⁺.

N-(3,5-bis(trifluoromethyl)phenyl)-2-(pyridin-2-ylthio)acetamide (2c)

Yield 57.4%; m.p. 110.6–111.7 °C; IR(KBr, cm⁻¹): 3431 (NH), 1669 (C = O); ¹H NMR (400 MHz, CDCl₃): δ (ppm) 3.88 (s, 2H, -CH₂), 7.21–7.26 (q, 1H, Pyridine-H₅, *J* = 5.2 Hz), 7.35–7.37 (d, 1H, Pyridine-H₃, *J* = 8.0 Hz), 7.55(s, 1H, Ph-H₄), 7.62–7.66 (m, 1H, Pyridine-H₄), 7.98 (s, 2H, Ph-H_{2,6}), 8.56–8.57 (d, 1H, Pyridine-H₆, *J* = 5.2 Hz), 10.94(s, 1H, NH); MS (ESI) *m/z* (%): 381.0 [M+H]⁺, 403.0 [M+Na]⁺.

N-(4,6-di-methoxy-pyrimidin-2-yl)-2-(pyridin-2-ylthio)acetamide (2d)

Yield 87.4%; m.p. 117.6–118.5 °C; IR(KBr, cm⁻¹): 3433 (NH), 1678 (C = O); ¹H NMR (400 MHz, CDCl₃): δ (ppm) 3.92 (s, 6H, 2 × OCH₃), 4.16 (s, 2H, -CH₂), 5.75 (s, 1H, ArH), 7.08–7.11 (q, 1H, Pyridine-H₅, *J* = 5.2 Hz), 7.30–7.32 (d, 1H, Pyridine-H₃, *J* = 8.0 Hz), 7.55–7.59

(m, 1H, Pyridine-H₄), 8.50–8.51(d, 1H, Pyridine-H₆, *J* = 3.6 Hz), 10.34 (s, 1H, NH); MS (ESI) *m/z* (%): 307.0 [M+H]⁺, 329.0 [M+Na]⁺, 345.0 [M+K]⁺.

2-(1H-benzo[d]imidazol-2-ylthio)-N-phenylacetamide (3a)

Yield 86.2%; m.p. 199.1–200.5 °C; IR (KBr, cm⁻¹): 3436 (NH), 1677 (C = O); ¹H NMR (400 MHz, CDCl₃): δ (ppm) 4.28 (s, 2H, -CH₂), 7.04–7.08 (t, 1H, PhCH-*p*, *J* = 7.6 Hz), 7.11–7.15 (m, 2H, PhCH-*m*), 7.29–7.33 (t, 2H, PhCH-*o*, *J* = 8.0 Hz), 7.41–7.51 (d, 2H, 2-Ph-H_{4,5}, *J* = 5.6 Hz), 7.57–7.60 (d, 2H, 2-Ph-H_{3,6}, *J* = 8.0 Hz), 10.51 (s, 1H, Imidazole-H), 12.66 (s, 1H, NH); MS (ESI) *m/z* (%): 281.9 [M-H]⁻.

2-(1H-benzo[d]imidazol-2-ylthio)-N-(2,5-di-fluoro-phenyl)acetamide (3b)

Yield 86.8%; m.p. 193.0–194.8 °C; IR (KBr, cm⁻¹): 3432 (NH), 1679 (C = O); ¹H NMR (400 MHz, CDCl₃): δ (ppm) 4.13 (s, 2H, -CH₂), 6.79–6.85 (m, 1H, Ph-H₄), 7.17–7.25 (m, 3H, 2-Ph-H_{4,5}, Ph-H₃), 7.56 (d, 2H, 2-Ph-H_{3,6}, *J* = 4.7 Hz), 8.23–8.28 (m, 1H, Ph-H₆), 11.60 (s, 1H, Imidazole-H), 11.84 (s, 1H, NH); MS (ESI) *m/z* (%): 317.9 [M-H]⁻.

2-(1H-benzo[d]imidazol-2-ylthio)-N-(3,5-bis(trifluoromethyl)phenyl)acetamide (3c)

Yield 89.2%; m.p. 202.4–203.8 °C; IR (KBr, cm⁻¹): 3432 (NH), 1680 (C = O); ¹H NMR (400 MHz, CDCl₃): δ (ppm) 4.34 (s, 2H, -CH₂), 7.11–7.15 (m, 2H, 2-Ph-H_{4,5}), 7.42–7.47 (t, 2H, 2-Ph-H_{3,6}, *J* = 18.2, 1.4 Hz), 7.79 (s, 1H, Ph-H₄), 8.25 (s, 2H, Ph-H_{2,6}), 11.14 (s, 1H, Imidazole-H), 12.69 (s, 1H, NH); MS (ESI) *m/z* (%): 418.0 [M-H]⁻.

2-(5-amino-1,3,4-thiadiazol-2-ylthio)-N-phenylacetamide (4a)

Yield 76.2%; m.p. 174.4–175.6 °C; IR (KBr, cm⁻¹): 3300 (NH), 1665 (C = O), 1629 (C = N); ¹H NMR (400 MHz, CDCl₃): δ (ppm) 3.99 (s, 2H, -CH₂), 7.05–7.09 (t, 1H, PhCH-*p*, *J* = 7.4 Hz), 7.30–7.34 (m, 4H, Ph-H), 7.56–7.58 (d, 2H, -NH₂, *J* = 7.6 Hz), 10.25 (s, 1H, NH); MS (ESI) *m/z* (%): 288.9 [M+Na]⁺, 304.9 [M+K]⁺.

2-(5-amino-1,3,4-thiadiazol-2-ylthio)-N-(2,5-di-fluorophenyl)acetamide (4b)

Yield 81.1%; m.p. 179.3–180.2 °C; IR (KBr, cm⁻¹): 3306 (NH), 1672 (C = O), 1629 (C = N); ¹H NMR (400 MHz, CDCl₃): δ (ppm) 4.11 (s, 2H, -CH₂), 6.69 (s, 2H, -NH₂), 6.85–6.91 (m, 1H, Ph-H₄), 7.19–7.26 (m, 1H, Ph-H₃), 8.13–8.18 (m, 1H, Ph-H₆), 9.81 (s, 1H, NH); MS (ESI) *m/z* (%): 301.0 [M+H]⁺, 324.9 [M+Na]⁺, 340.9 [M+K]⁺.

2-(5-amino-1,3,4-thiadiazol-2-ylthio)-N-(3,5-bis(trifluoromethyl)phenyl)acetamide (4c)

Yield 82.2%; m.p. 184.2–185.9 °C; IR(KBr, cm⁻¹): 3489 (NH), 1698 (C = O), 1615 (C = N); ¹H NMR (400 MHz, CDCl₃): δ (ppm) 4.10 (s, 2H, -CH₂), 6.72 (s, 2H, -NH₂), 7.73 (s, 1H, Ph-H₄), 8.29 (s, 2H, Ph-H_{2,6}), 10.26 (s, 1H, NH); MS (ESI) *m/z* (%): 424.9 [M+Na]⁺, 440.9 [M+K]⁺.

2-(5-amino-1,3,4-thiadiazol-2-ylthio)-*N*-(4,6-dimethoxy-pyrimidin-2-yl)acetamide (4d)

Yield 89.3%; m.p. 187.1–188.5 °C; IR (KBr, cm^{-1}): 3462 (N-H), 1667 (C = O), 1630 (C = N); ^1H NMR (400 MHz, CDCl_3): δ (ppm) 3.88 (s, 6H, $2 \times \text{OCH}_3$), 4.38 (s, 2H, $-\text{CH}_2$), 5.93 (s, 1H, ArH), 7.29 (s, 2H, NH_2), 10.69 (s, 1H, NH); MS (ESI) m/z (%): 329.0 $[\text{M}+\text{H}]^+$, 350.9 $[\text{M}+\text{Na}]^+$, 366.9 $[\text{M}+\text{K}]^+$.

In vitro assays of anti-HIV activity

The inhibitory activity of the test compounds on HIV-1 IIIB replication in MT-4 was based on the quantitative detection of HIV-1 p24 core antigen in the culture supernatant, which was determined with enzyme-linked immunosorbent assay (ELISA) by Vironostika HIV-1 Antigen MicroELisa Assay (Organon Teknika, Dublin, Ireland), according to the manufacturer's protocol. In brief, 1×10^4 MT-4 cells in 96-well plates were infected with HIV-1 IIIB (100 TCID_{50}) in the presence or absence of a test compound at graded concentrations, followed by incubation at 37 °C overnight. Then, the culture supernatants were removed, and fresh media containing no test compounds were added. After 2 days of cultivation, the medium was removed and the cells were fixed with 100 μL of phosphate-buffered saline (PBS) containing 1% formaldehyde and 0.2% glutaraldehyde for 5 min at room temperature. The cells were then washed three times with PBS and incubated for 1 h at 37 °C with 100 μL of an indicator HRP. The reaction was terminated by addition of 1N H_2SO_4 . Absorbance at 450 nm was recorded in an ELISA reader. Recombinant protein p24 was included for establishing standard dose–response curves. Each sample was tested in triplicate.

Molecular modeling study

The automated docking studies were performed with AutoDock 4.0 (20). This automated ligand-docking program uses the Lamarckian genetic algorithm (LGA) to explore the full range of ligand conformational flexibility with partial flexibility of the receptor. Lamarckian genetic algorithm is a hybrid of a genetic algorithm and a local search algorithm. This algorithm first builds a population of individuals (genes), each gene being a different random conformation of the docked compound. The local search algorithm then performs energy minimizations on a user-specified proportion of the population of individuals. If the energy of the new individual is lower than that of the old, the new one is automatically accepted as the next step in docking.

Preparation of the receptor and ligands molecules

The three-dimensional structures of ligands were constructed using standard bond lengths and bond angles of the GaussView 3.09 software (Gaussian, Inc., Wallingford, CT, USA). Geometry optimizations were carried out with the semi-empirical AM1 method, and then output files were minimized by using density functional (DFT) method by applying the B3LYP (Becke, Lee, Yang and Parr) correlation functional in the second optimization. Gasteiger partial charges were assigned using the AutoDock Tools. The crystal structure of HIV-1 RT receptor in complex with PTT (*N*-(5-chloro-2-pyridinyl)-*N'*-[2-(4-ethoxy-3-fluoro-2-pyridinyl)ethyl]-thiourea) was retrieved from

the Brookhaven Protein Data Bank (PDB entry code 1dtt). After the removal of the inhibitor from the complex, polar hydrogen atoms and the Kollman-united charges were added to the macromolecule.

Molecular modeling and analysis of the docked results

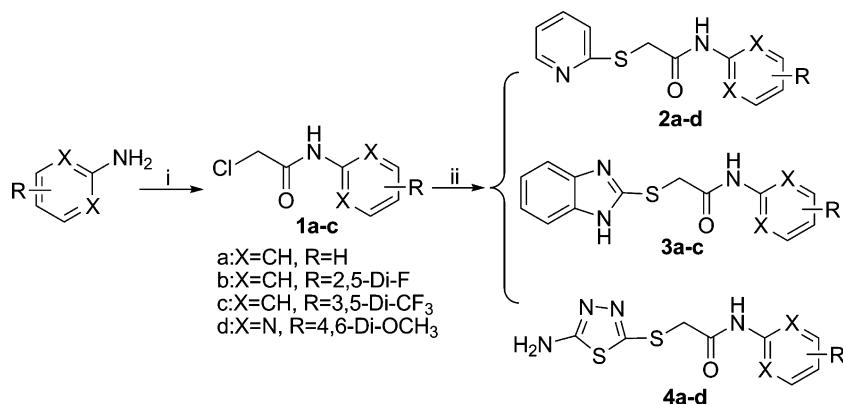
For the docking, a grid spacing of 0.375 Å and $61 \times 61 \times 61$ number of points were used. Given the known location of the NNRTI-binding site, the cubic grid box was centered in the catalytic active region and encompassed the binding site, and the grid center was designated at dimensions (x , y and z): -1.121 , -34.649 and 23.964 . Docked conformations were generated using the LGA with an initial population size of 150 structures. Further parameters were set to their default values. For docking assessment, the same docking protocol was used on the reference drug PTT. AutoDock successfully reproduced the bound conformation with a RMSD value of only 1.31 Å. The first-ranked docked conformation (Best Docked conformation) and the lowest-energy conformation of the most populated cluster (Best Cluster conformation) were selected as the binding conformation. Model analyses were performed using the Accelrys DS Visualizer 2.0 software (Accelrys, Inc., San Diego, CA, USA).

Results and Discussion**Chemistry**

The *N*-aryl-2-arylthioacetamide derivatives were synthesized using the conventional strategy as depicted in Scheme 1. The starting compound, 2-chloro-*N*-substituted-acetamides (**1**), was readily synthesized by the reaction of chloroacetyl chloride and anilines or pyrimidinylamines in acetic acid at ambient temperature in 75–95% yields (21). By alkylation of the corresponding sodium thiolate with **1**, we prepared *N*-aryl-2-arylthioacetamide derivatives **2–4**. At the alkylation reactions, the literature procedure (22) was carried out for several hours in ethanol. Our more versatile procedure used KI as the catalyst, which afforded the *N*-aryl-2-arylthioacetamides in good yields and with short reaction times. The **2–4** were isolated in 51–89% yields (Table 1) as colorless powders, which were generally purified by recrystallization with CH_2Cl_2 and petroleum ether. The structures of **2–4** were determined by the IR, NMR and mass spectra. The **1a–d** were confirmed in particular by the presence of a proton of NH as a singlet signal at 8.30–9.62 ppm in ^1H NMR spectra. The IR spectrum of the *N*-aryl-2-arylthioacetamide derivatives (**2–4**) contained a characteristic absorption band of the CONH group at 1665–1700 and 3300–3460/ cm . The ^1H NMR spectra of **2–4**, containing the thiomethylene group, revealed the SCH_2 protons at 3.88–4.38 ppm. In addition, the ESI–MS spectra of **2–4** exhibited the anticipated molecular ion peaks, and the fragmentation ions were consistent with their structures.

Biological activity

The inhibitory activity of *N*-aryl-2-arylthioacetamide derivatives **2–4** was evaluated against HIV-1 (IIIB) replication in MT-4 cell culture using ELISA (23,24). The compound Zidovudine (azidothymidine, AZT) was used as a reference drug. The results, expressed as IC_{50} values, are summarized in Table 1. Although the tested compounds



Scheme 1: General preparation of *N*-aryl-2-arylthioacetamides (**2–4**). Reagents and conditions: (i) chloroacetyl chloride, AcOH, 0 °C → rt, 4 h; (ii) thiol, NaOH, EtOH, KI, rt, 1 h.

Table 1: Preparation of **2a–d**, **3a–c** and **4a–d** and anti-HIV-1 activity values^a

Compound	X	R	Mp (°C)	Yield (%)	IC ₅₀ (μM) ^b
2a	CH	H	61.3–62.9	87.5	>100
2b	CH	2,5-di-F	112.5–113.8	50.6	>100
2c	CH	3,5-di-CF ₃	110.6–111.7	57.4	>100
2d	N	4,6-di-OCH ₃	117.6–118.5	87.4	>100
3a	CH	H	199.1–200.5	86.2	5.07 ± 0.21
3b	CH	2,5-di-F	193.0–194.8	86.8	1.25 ± 0.08
3c	CH	3,5-di-CF ₃	202.4–203.8	89.2	2.20 ± 0.32
4a	CH	H	174.4–175.6	76.2	20.83 ± 1.17
4b	CH	2,5-di-F	179.3–180.2	81.1	16.10 ± 0.24
4c	CH	3,5-di-CF ₃	184.2–185.9	82.2	14.93 ± 0.84
4d	N	4,6-di-OCH ₃	187.1–188.5	89.3	7.50 ± 1.06

^aZidovudine was used as a reference compound; IC₅₀ for zidovudine was 0.016 μM.

^bCompound concentration required to decrease the viability of mock-infected cells by 50%; Data represent mean values for three separate experiments, variation among triplicate samples was <15%.

exhibited less anti-HIV-1 activities than that of AZT (IC₅₀ = 0.016 μM) as the control, the majority of them were active in the lower micromolar concentration (1.25–20.83 μM), appreciably revealing their promising potential inhibitory activities.

It has been observed that the electronic properties of the arylthio substituents significantly affected the activity compared to the *N*-aryl substituents. Among them, analogs of **3** series showed IC₅₀ values <5.07 μM. Compound **3b** was the most active one with the highest potency (IC₅₀ = 1.25 μM) lower than the reference drug of AZT, which indicates that the 1*H*-benzo[*d*]imidazole is an acceptable isosteric replacement for the triazole in the lead compound **A**. Interestingly, the activities of 1*H*-benzo[*d*]imidazoles **3a–c** were turned out to be the most potent *N*-aryl-2-arylthioacetamides compared to the corresponding pyridines **2a–d** and 5-amino-1,3,4-thiadiazoles **4a–d** (**3a** versus **2a** and **4a**; **3b** versus **2b** and **4b**; **3c** versus **2c** and **4c**).

The electronic properties of groups on the *N*-aryl affected the antiviral potency of **2–4**. The introduction of fluorine atoms or tr-

omethyl groups on the *N*-phenyl ring improved antiviral potency, whereas their unsubstituted *N*-phenyl series led to less potent derivatives in both 1*H*-benzo[*d*]imidazole and 5-amino-1,3,4-thiadiazole series (compare **3b,c** with **3a**, and **4b,c** with **4a**). It is appeared to confirm our assumption that the analogs bearing an electron-withdrawing group might be more potent than the congeners with an electron-donating group. Interestingly, the 2,5-difluoro derivative **3b** was two times more potent than 3,5-difluoromethyl compound **3c**, and the same replacement of **4b** was led to a decrease in potency with respect to the 3,5-difluoromethyl compound **4c**. The activity trend suggested that the steric/electronic properties of the *N*-phenyl substituents influenced the antiretroviral activity more than how their positions do.

Successively, the type of rings on the *N*-aryl also affected the antiviral potency of **2–4**. **4d** with heteroaryl ring was indicated the highest anti-HIV activity in the **4** series, probably because the 4,6-dimethoxy-pyrimidyl ring might be more favorable to improve a putative π -stacking interaction between the electron-deficient aryl ring of the ligand and the electron-rich benzene ring of RT (25).

Molecular docking studies

In attempt to further elucidate the high HIV-1 inhibitory potencies of the **2–4** at a molecular level, the computer-simulated automated docking studies were performed using the widely distributed molecular docking software, AutoDock, which has been successfully used to predict protein recognition and binding (26–28). The HIV-1 RT/NNRTI complexes of X-ray crystallography had identified that the NNRTIs show a common configuration resembling a butterfly-like shape where the wings generally contain aromatic rings that have π - π interactions with aromatic amino acid residues (29–33). All test compounds **2–4** were docked into the NNBS using the recently published HIV-1 RT protein crystal structure of PETT (PDB entry code 1dtl) as template (29). Prior to automate docking of the reported inhibitors, PETT itself was docked into the HIV-1 RT crystal

structure as a means of testing program performance. A superposition of the most highly scored conformation of the ligand onto its crystallographic geometry yielded a RMSD (root mean square deviation) of 1.31 Å, which was the best docked conformation by <2 Å (34), thus revealing that AutoDock was successful in reproducing the binding mode of PETT into the active site of HIV-1 RT.

Two different interactional modes of **3b** and **4d** with the RT receptor were generated from docking. In the most frequently occurring and most favorable result, **3b** was found to bind the NNBS in an orientation very similar to that of the co-crystallized inhibitor PETT, and compound **4d** displayed a different binding mode. Figure 3 shows the predicted binding mode of **3b** and **4d** to the active site of HIV-1 RT. A schematic depiction of the interaction between both

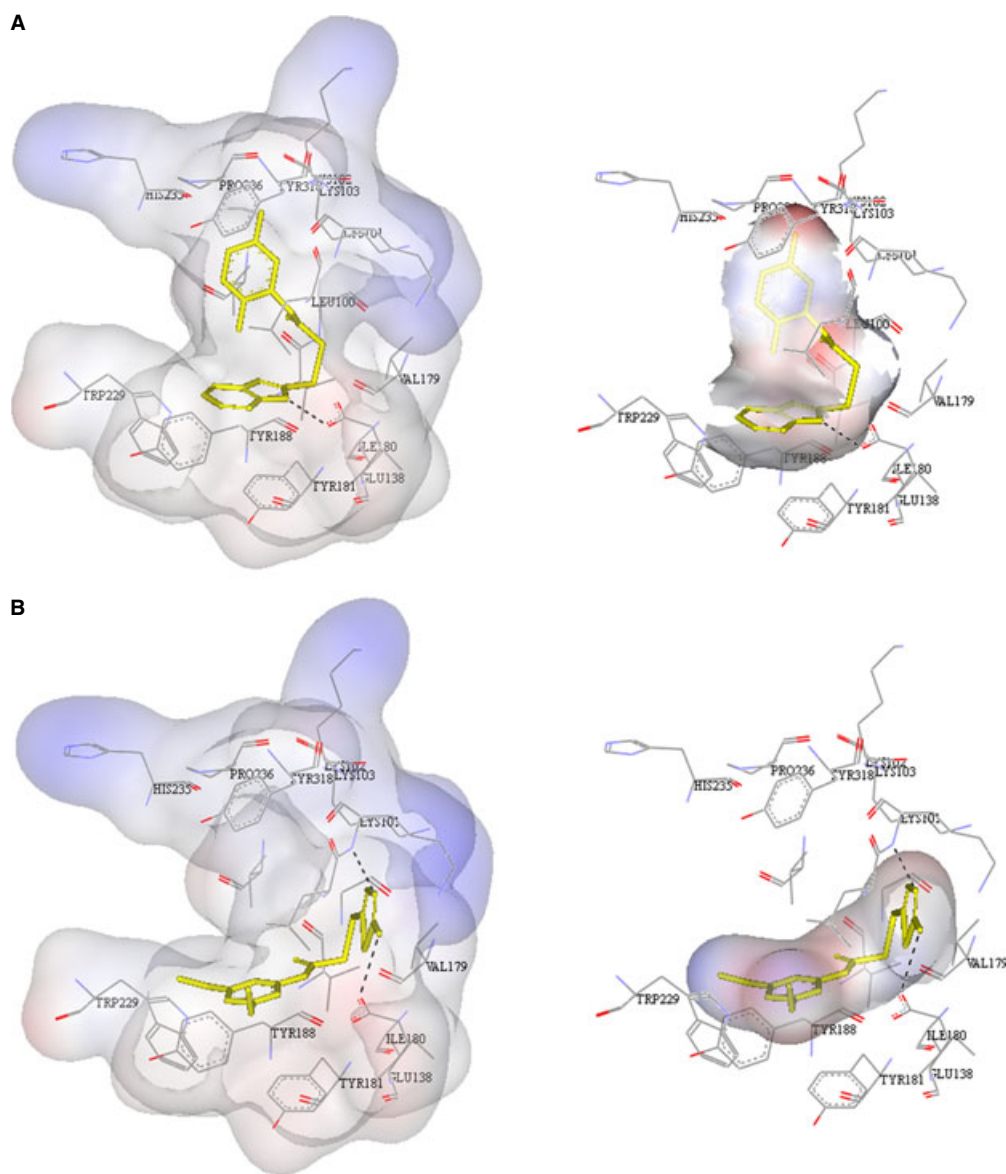


Figure 3: Stereographic views of the binding mode of compounds (A) **3b** and (B) **4d** in the HIV-1 RT NNBS. The ligands are represented as bold sticks, while the amino acid residues lining the RT NNBS are shown as thin sticks. For clarity, only interacting polar hydrogen atoms are displayed. Hydrogen bonds are depicted as dashed lines.

inhibitors and the RT NNBS residues is illustrated in Figure 4. It can be observed from Figure 3A that the NH function of the 1*H*-benzo[*d*]-imidazole of **3b** makes a hydrogen bond with the main chain carbonyl oxygen of Glu138 ($\text{NH}\cdots\text{O} = \text{C}$, $d = 2.08 \text{ \AA}$), whereas compound **4d** is involved in two hydrogen bonds with the enzyme backbone: one involves the amino group of thiadiazole and the carbonyl oxygen of Glu138 ($\text{NH}\cdots\text{O} = \text{C}$, $d = 2.20 \text{ \AA}$) and the other occurs between the nitrogen of thiadiazole and the main chain NH group of Lys101 ($\text{N}\cdots\text{HN}$, $d = 1.82 \text{ \AA}$).

In comparing the docking simulations of **2a–d** with that of **3b** and **4d** in the NNBS, we did not observe any H-bonding interaction between the nitrogen of pyridine and the enzyme. The lack of this hydrogen bond prevents the ligand from assuming a bioactive U-shaped conformation within the NNBS, and this is consistent with

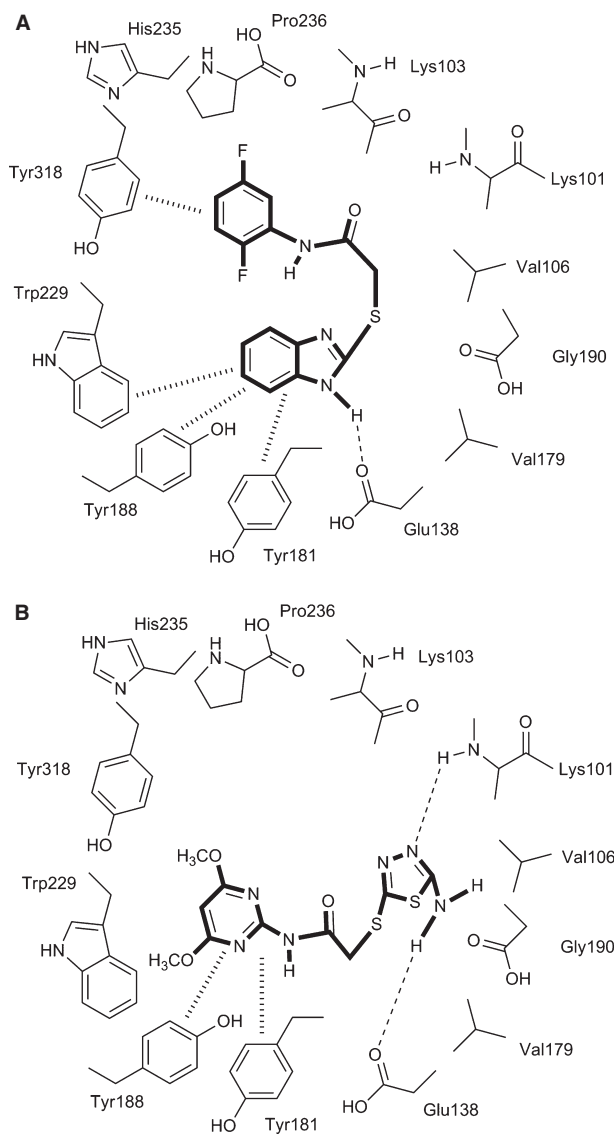


Figure 4: Schematic diagrams showing the intermolecular interactions between the inhibitors (A) **3b**, (B) **4d**, and the surrounding residues of HIV-1 RT NNBS. NNBS, non-nucleoside binding site.

the biological data, which shows that **3b** and **4d** are more potent than **2**.

As shown in Figure 4A, the thiomethyl linker of the RT/**3b** complex is embedded within a hydrophobic pocket made up by the side chains of Val106 and Val179, while the 1*H*-benzo[*d*]-imidazole moiety fills the hydrophobic bottom of the NNBS made up by the aromatic rings of Tyr181, Tyr188 and Trp229 as well as by Glu138. In particular, it is involved in π - π interactions with Tyr181, Tyr188 and interacts with a tilted T contact with the aromatic indole nucleus of Trp229. Furthermore, the favorable steric interactions of the *N*-phenyl ring with a hydrophobic pocket are defined by the side chains of the Leu100, Lys103, His235 and Tyr318. The fluorine atom establishes van der Waals contacts with the Pro236 main chain atoms, and the imidic oxygen is involved in a network of polar interactions with the Leu100 main chains, thus providing further stabilization to the complex.

Interestingly, the conformation of compound **4d** in Figure 4B lies along the RT NNBS in opposite direction to that of **3b**. The pyrimidine ring establishes the π - π interactions with the Tyr181 and Tyr188 side chain, whereas the thiadiazole group is involved in van der Waals interactions with Val179, Lys101 and Gly190. Notably, the model shows the formation of two potential intermolecular hydrogen bonds, which is one more than that of **3b**.

This additional hydrogen bond might explain not only the same level of antiviral activity of **3b** through a stable interaction with RT but also its reverse binding mode to the NNBS. In fact, if their binding modes were similar, the thiadiazole group should be located at the bottom of the RT pocket, as above said for the 1*H*-benzo[*d*]-imidazole ring of **3b**. As a consequence, this moiety would not be suitably situated to form the hydrogen bond with Lys101. The reverse binding mode of **4d** cannot approximate the butterfly-like structure commonly observed with other NNRTIs (29), but it is compensated by the number of hydrophobic contacts and more hydrogen bonds in which **4d** is engaged.

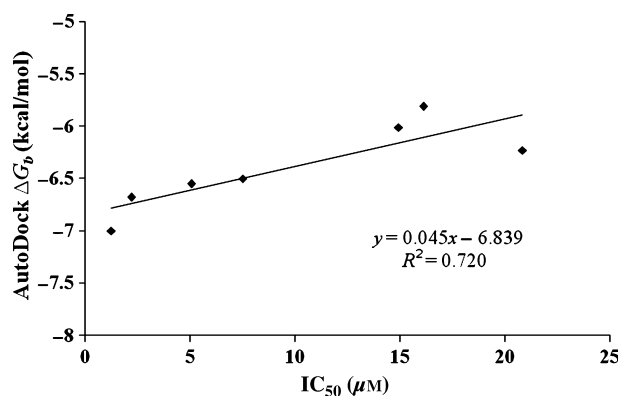
Inspection of the RT/**3b** complex revealed that the *N*-phenyl ring is hosted in a subpocket, made up by the side chains of Leu100, Lys103, His235 and Tyr318. Notably, these residues are involved through prominent van der Waals and π - π stacking interactions, with the π -electron systems located in the butterfly wings of RT NNBS conformation (30,32). We hypothesized that an efficient occupancy of this region by strategically designed aromatic substituents should yield more potent anti-HIV-1 agents with higher affinity for the RT binding pocket. Actually, the analog **3b** and **3c** were four-fold and twofold more active than **3a**, respectively, suggesting that there is a wide sterically allowed usable space in the regions hosting the *N*-phenyl and the (hetero)aryl moieties. These observations could provide the basis for further structural modifications of them.

Binding affinities

The binding affinity was evaluated by the binding free energies (ΔG_b), inhibition constants (K_i) and hydrogen bonding values. The compounds **2–4** which revealed the highest binding affinities, that is, the lowest binding free energies, within HIV-1 RT NNBS and the

Table 2: The best docking results based on the binding free energies (ΔG_b) and inhibition constants (K_i) of **2–4**

Compound	ΔG_b^a (kcal/mol)	K_i^b	Hydrogen bonds between atoms of compounds and amino acids				RMSD ^c (Å)
			Atom of compound	Amino acid	Distance (Å)	Angle (°)	
2a	-4.76	3.26E-4	–	–	–	–	7.32
2b	-5.73	6.26E-5	–	–	–	–	4.63
2c	-5.57	8.22E-5	–	–	–	–	8.49
2d	-5.27	1.37E-4	–	–	–	–	5.69
3a	-6.55	1.59E-5	N ₁ -H	CO of Glu 138	2.03	162.1	7.85
3b	-7.00	7.35E-6	N ₁ -H	CO of Glu 138	2.08	154.5	8.76
3c	-6.68	1.27E-5	N ₁ -H	CO of Lys 101	1.77	169.7	8.75
4a	-6.23	2.69E-5	–	–	–	–	7.09
4b	-5.81	5.50E-5	–	–	–	–	5.67
4c	-6.01	3.96E-5	C ₅ -NH	CO of Gly 99	2.15	142.4	6.51
			C ₅ -NH	CO of Glu 138	2.20	159.4	
			N ₁	HN of Lys 101	1.78	145.3	
4d	-6.50	7.83E-5	C ₅ -NH	CO of Glu 138	2.20	135.3	3.80
			N ₁	HN of Lys 101	1.82	160.5	
PETT ^d	-6.07	3.57E-5	N ₈ -H	CO of Lys 101	2.16	124.6	1.31

^aBinding free energy.^bInhibition constant.^cRoot mean square deviation.^dThe native co-crystallized bound ligand (PETT) of HIV-1 RT (PDB code: 1dtl).**Figure 5:** Correlation between the ΔG_b and IC_{50} of **3a–c** and **4a–d**.

hydrogen bond interactions into the target macromolecule, are represented in Table 2. The **3** series exhibited the lowest free energy between -7.00 and -6.55 kcal/mol and **3b** with the least binding free energy (-7.00 kcal/mol) by fitting well into the groove of the binding site. The overall correlation between the inhibitory activities (IC_{50} , μM) of the *N*-aryl-2-arylthioacetamids **2–4** and the binding affinities (lower binding free energy) predicted by AutoDock was fairly good for some compounds. Especially, the correlation between the binding free energy (ΔG_b) and IC_{50} (μM) values for compounds **3a–c** and **4a–d** revealed a correlation coefficient (R^2) of 0.720 as shown in Figure 5.

Conclusions

N-aryl-2-arylthioacetamides **2–4** were designed and synthesized as a new class of NNRTIs, taking into account the 'butterfly-like'

conformation as a determinant requisite for antiretroviral activity. These compounds showed significant anti-HIV-1 activity in the micromolar concentration range (1.25 – 20.83 μM). Compounds **3a–c** turned out to be the most potent derivatives compared to **2a–d** and **4a–d**, by the replacement of the pyridine or thiazazole ring of the arylthio moiety with 1*H*-benzo[*d*]imidazole. In particular, introduction of fluorine atoms or trifluoromethyl groups on the *N*-phenyl ring of **3** series was endowed with high activity and selectivity. The most potent **3b** displayed an IC_{50} value of 1.25 μM lower than that of the lead compound **A**.

Molecular modeling and docking studies were employed to understand the interactions between these inhibitors and the reverse transcriptase. The highest potency of **3b** would be ascribable to the stabilization by the hydrogen bond between the NH of the 1*H*-benzo[*d*]imidazole and the Glu138 main chain carbonyl and van der Waals contacts between the *N*-phenyl ring and the Leu100, Lys103, His235 and Tyr318 side chains, which bind to reverse transcriptase assuming a 'butterfly-like' orientation. Finally, considering the binding affinities and conformations of **3** series, further SAR studies, keeping constant the *N*-phenyl and the (hetero)aryl substitution patterns emerged as the best in the present work, will be the object of the following paper.

Acknowledgments

This work was financially supported by Key Projects in the National Science & Technology Pillar Program during the Eleventh Five-Year Plan Period (No. 2008ZX10001-015) and Funding Project for Academic Human Resources Development in Institutions of Higher Learning under the Jurisdiction of Beijing Municipality. We thank Department of Viro-Pharmacology, Beijing University of Technology, for their assistances in the experiments.

References

- Mitsuya H., Broder S. (1987) Strategies for antiviral therapy in AIDS. *Nature*;325:773–778.
- De Clercq E. (1998) The role of non-nucleoside reverse transcriptase inhibitors (NNRTIs) in the therapy of HIV-1 infection. *Antiviral Res*;38:153–179.
- Stevens M., De Clercq E., Balzarini J. (2006) The regulation of HIV-1 transcription: molecular targets for chemotherapeutic intervention. *Med Chem Rev*;26:595–625.
- Meadows D.C., Gervay H.J. (2006) Current developments in HIV chemotherapy. *Chem Med Chem*;1:16–29.
- Spence R.A., Kati W.M., Anderson K.S., Johnson K.A. (1995) Mechanism of inhibition of HIV-1 reverse transcriptase by non-nucleoside inhibitors. *Science*;267:988–993.
- Barbaro G., Scozzafava A., Mastrolorenzo A., Supuran C.T. (2005) Highly active antiretroviral therapy: current state of the art new agents and their pharmacological interactions useful for improving therapeutic outcome. *Curr Pharm Des*;11:1805–1843.
- Koup R.A., Merluzzi V.J., Hargrave K.D., Adams J., Grozinger K., Eckner R.J., Sullivan J.L. (1991) Inhibition of human immunodeficiency virus type 1 (HIV-1) replication by the dipyrindodiazepinone BI-RG-587. *J Infect Dis*;163:966–970.
- Young S.D., Britcher S.F., Tran L.O., Payne L.S., Lumma W.C., Lyle T.A., Huff J.R. *et al.* (1995) L-743, 726 (DMP-266): a novel, highly potent nonnucleoside inhibitor of the human immunodeficiency virus type 1 reverse transcriptase. *Antimicrob Agents Chemother*;39:2602–2605.
- Freimuth W.W. (1996) Delavirdine mesylate, a potent non-nucleoside HIV-1 reverse transcriptase inhibitor. *Adv Exp Med Bio*;394:279–289.
- Pauwels R., Andries K., Desmyter J., Schols D., Kukla M.J., Breslin H.J., Raeymaeckers A., Van G.J., Woestenborghs R., Heykants J., Schellekens K., Janssen M.A.C., De Clercq E., Janssen P.A.J. (1990) Potent and selective inhibition of HIV-1 replication *in vitro* by a novel series of TIBO derivatives. *Nature*;343:470–474.
- Balzarini J., Pelemans H., Aquaro S., Perno C.F., Witvrouw M., Schols D., De Clercq E., Karlsson A. (1996) Highly favorable antiviral activity and resistance profile of the novel thiocarboxanilide pentenyloxy ether derivatives UC-781 and UC-82 as inhibitors of human immunodeficiency virus type 1 replication. *Mol Pharmacol*;50:394–401.
- Goldman M.E., Nunberg J.H., O'Brien J.A., Quintero J.C., Schleif W.A., Freund K.F., Gaul S.L., Saari W.S., Wai J.S., Hoffman J.M., Anderson P.S., Hupe D.J., Emini E.A., Stern A.M. (1991) Pyridinone derivatives: specific human immunodeficiency virus type 1 reverse transcriptase inhibitors with antiviral activity. *Proc Natl Acad Sci USA*;88:6863–6867.
- Patel M., Ko S.S., McHugh R.J.J., Markwalder J.A., Srivastava A.S., Cordova B.C., Klabe R.M., Erickson-Viitanen S., Trainor G.L., Seitz S.P. (1999) Synthesis and evaluation of analogs of Efavirenz (SUSTIVA) as HIV-1 reverse transcriptase inhibitors. *Bioorg Med Chem Lett*;9:2805–2810.
- De Clercq E. (1999) Perspectives of non-nucleoside reverse transcriptase inhibitors (NNRTIs) in the therapy of HIV-1 infection. *Farmacol*;54:26–45.
- Iilina T., Parniak M.A. (2008) Inhibitors of HIV-1 reverse transcriptase. *Adv Pharmacol*;56:121–167.
- Wang Z., Wu B., Kuhen K.L., Bursulaya B., Nguyen T.N., Nguyen D.G., He Y. (2006) Synthesis and biological evaluations of sulfanyltriazoles as novel HIV-1 non-nucleoside reverse transcriptase inhibitors. *Bioorg Med Chem Lett*;16:4174–4177.
- Muraglia E., Kinzel O.D., Laufer R., Miller M.D., Moyer G., Munshi V., Orvieto F., Palumbi M.C., Pescatore G., Rowley M., Williams P.D., Summa V. (2006) Tetrazole thioacetanilides: potent non-nucleoside inhibitors of WT HIV reverse transcriptase and its K103N mutant. *Bioorg Med Chem Lett*;16:2748–2752.
- Zhan P., Liu X., Cao Y., Wang Y., Pannecouque C., De Clercq E. (2008) 123-Thiadiazole thioacetanilides as a novel class of potent HIV-1 non-nucleoside reverse transcriptase inhibitors. *Bioorg Med Chem Lett*;18:5368–5371.
- Zhang Z., Xu W., Koh Y.H., Shim J.H., Girardet J.L., Yeh L.T., Hamatake R.K., Hong Z. (2007) A novel nonnucleoside analogue that inhibits human immunodeficiency virus type 1 isolates resistant to current nonnucleoside reverse transcriptase inhibitors. *Antimicrob Agents Chemother*;51:429–437.
- Hu R., Barbault F., Delamar M., Zhang R. (2009) Receptor- and ligand-based 3D-QSAR study for a series of non-nucleoside HIV-1 reverse transcriptase inhibitors. *Bioorg Med Chem*;17:2400–2409.
- Yong S.R., Ung A.T., Pyne S.G., Skelton B.W., White A.H. (2007) Synthesis of novel 3'-spirocyclic-oxindole derivatives and assessment of their cytostatic activities. *Tetrahedron*;63:5579–5586.
- Rodinovskaya L.A., Shestopalov A.M., Gromova A.V., Shestopalov A.A. (2008) One-pot synthesis of diverse 4-di(tri)fluoromethyl-3-cyanopyridine-2(1H)-thiones and their utilities in the cascade synthesis of annulated heterocycles. *J Comb Chem*;10:313–322.
- Liu K., Lu H., Hou L., Qi Z., Teixeira C., Barbault F., Fan B.T., Liu S., Jiang S., Xie L. (2008) Design, synthesis, and biological evaluation of *N*-carboxyphenylpyrrole derivatives as potent HIV fusion inhibitors targeting gp41. *J Med Chem*;51:7843–7854.
- Kanamoto T., Kashiwada Y., Kanbara K., Gotoh K., Yoshimori M., Goto T., Sano K., Nakashima H. (2001) Anti-human immunodeficiency virus activity of YK-FH312 (a betulinic acid derivative), a novel compound blocking viral maturation. *Antimicrob Agents Chemother*;45:1225–1230.
- Silvestri R., Artico M., De Martino G., Ragno R., Massa S., Lodo R., Murgioni C., Loi A.G., La Colla P., Pani A. (2002) Synthesis, biological evaluation, and binding mode of novel 1-[2-(diarylmethoxy)ethyl]-2-methyl-5-nitroimidazoles targeted at the HIV-1 reverse transcriptase. *J Med Chem*;45:1567–1576.
- De Martino G., La Regina G., Di Pasquali A., Ragno R., Bergamini A., Ciapri C., Sinistro A., Maga G., Crespan E., Artico M., Silvestri R. (2005) Novel 1-[2-(diarylmethoxy)ethyl]-2-methyl-5-nitroimidazoles as HIV-1 non-nucleoside reverse transcriptase inhibitors. *J Med Chem*;48:4378–4388.
- Shrestha A.R., Ali H.I., Ashida N., Nagamatsu T. (2008) Antitumor studies, part 5: synthesis antitumor activity and molecular docking study of 5-(monosubstituted amino)-2-deoxy-2-phenyl-5-deazaflavins. *Bioorg Med Chem*;16:9161–9170.
- Kovac A., Konc J., Vehar B., Bostock J.M., Chopra I., Janezic D., Gobec S. (2008) Discovery of new inhibitors of D-Alanine ligase by structure-based virtual screening. *J Med Chem*;51:7442–7448.

29. Ding J., Das K., Tantillo C., Zhang W., Clark A.D.J., Jessen S., Lu X. *et al.* (1995) Structure of HIV-1 reverse transcriptase in a complex with the non-nucleoside inhibitor α -APA R95845 at 2.8 Å resolution. *Structure*;3:365–379.
30. Ren J., Diprose J., Warren J., Esnouf R.M., Bird L.E., Ikemizu S., Slater M., Milton J., Balzarini J., Stuart D.I., Stammers D.K. (2000) Phenylethylthiazolylthiourea (PETT) non-nucleoside inhibitors of HIV-1 and HIV-2 reverse transcriptases: structural and biochemical analyses. *J Biol Chem*;275:5633–5639.
31. Schafer W., Friebe W.G., Leinert H., Mertens A., Poll T., von der Saal W., Zilch H., Nuber B., Ziegler M.L. (1993) Non-nucleoside inhibitors of HIV-1 reverse transcriptase: molecular modeling and X-ray structure investigations. *J Med Chem*;36:726–732.
32. Jonckheere H., Anne J., De Clercq E. (2000) The HIV-1 reverse transcription (RT) process as target for RT inhibitors. *Med Res Rev*;20:129–154.
33. Richman D.D., Morton S.C., Wrin T., Hellmann N., Berry S., Shapiro M.F., Bozzette S.A. (2004) The prevalence of antiretroviral drug resistance in the United States. *AIDS*;18:1393–1401.
34. Paul M.K., Mukhopadhyay A.K. (2004) Tyrosine kinase-role and significance in cancer. *Int J Med Sci*;1:101–115.